Correlation between the Josephson coupling energy and the condensation energy in bilayer cuprate superconductors

Dominik Munzar,[1,2] Christian Bernhard,[2] Todd Holden,[2] Andrzej Golnik,[2,*] Josef Humlíček,[1] and Manuel Cardona[2]
[1]*Department of Solid State Physics, Faculty of Science, Masaryk University, Kotlářská 2, CZ-61137 Brno, Czech Republic*
[2]*Max-Planck-Institut für Festkörperforschung, Heisenbergstrasse 1, D-70569 Stuttgart, Germany*
(Received 1 September 2000; revised manuscript received 6 March 2001; published 21 June 2001)

We review some previous studies concerning the intrabilayer Josephson plasmons and present ellipsometric data of the *c*-axis infrared response of almost optimally doped $Bi_2Sr_2CaCu_2O_8$. The *c*-axis conductivity of this compound exhibits the same kind of anomalies as that of underdoped $YBa_2Cu_3O_{7-\delta}$. We analyze these anomalies in detail and show that they can be explained within a model involving the intrabilayer Josephson effect and variations of the electric field inside the unit cell. The Josephson coupling energies of different bilayer compounds obtained from the optical data are compared with the condensation energies and it is shown that there is a reasonable agreement between the values of the two quantities. We argue that the Josephson coupling energy, as determined by the frequency of the intrabilayer Josephson plasmon, represents a reasonable estimate of the change of the effective *c*-axis kinetic energy upon entering the superconducting state. It is further explained that this is not the case for the estimate based on the use of the simplest ''tight-binding'' sum rule. We discuss possible interpretations of the remarkable agreement between the Josephson coupling energies and the condensation energies. The most plausible interpretation is that the interlayer tunneling of the Cooper pairs provides the dominant contribution to the condensation energy of the bilayer compounds; in other words that the condensation energy of these compounds can be accounted for by the interlayer tunneling theory. We suggest an extension of this theory, which may also explain the high values of T_c in the single-layer compounds $Tl_2Ba_2CuO_6$ and $HgBa_2CuO_4$, and we make several experimentally verifiable predictions.

DOI: 10.1103/PhysRevB.64.024523 PACS number(s): 74.72.−h, 74.25.Gz, 74.20.Mn, 74.50.+r

I. INTRODUCTION

The interlayer tunneling (ILT) theory[1–3] provides a simple explanation of the surprisingly high values of T_c in the cuprate superconductors. It is based on the idea[1–4] that the pairing mechanism is substantially amplified by a decrease of the effective *c*-axis kinetic energy of the electrons upon entering the superconducting state. A prerequisite for this decrease is the absence (or at least a strong suppression) of the coherent single-particle tunneling between the copper-oxygen planes. The onset of the Cooper pair tunneling by the Josephson mechanism at T_c then leads to the decrease of the kinetic energy. According to the ILT theory, this gain of energy, which can be expressed[5] as the negatively taken coupling energy of the internal Josephson junctions (E_J), represents the dominant part of the condensation energy of the superconductor (U_0),

$$E_J \approx U_0 . \tag{1}$$

This relation, which should be exact in the limit of negligible in-plane contribution to the condensation energy and negligible coherent single-particle tunneling, has been shown to be only moderately violated for $La_{2-x}Sr_xCuO_4$ (Ref. 6) but strongly violated for $Tl_2Ba_2CuO_6$ (Tl-2201) (Refs. 6–9) and for $HgBa_2CuO_4$ (Hg-1201).[10] Here we show that Eq. (1) is fulfilled for two compounds that have two copper-oxygen planes per unit cell (bilayer compounds): $YBa_2Cu_3O_{7-\delta}$ (Y123) and $Bi_2Sr_2CaCu_2O_8$ (Bi-2212).

So far the relation (1) has been tested only for single-layer compounds, since it was not clear what kind of coupling takes place for the closely spaced copper-oxygen planes of the bilayer compounds. Anderson assumed that even these planes are only weakly coupled and argued that the bilayer compounds consist of two kinds of Josephson junctions: interbilayer and intrabilayer.[11] The Josephson plasma frequency of the interbilayer junction (ω_{int}) is lower than that of the intrabilayer junction (ω_{bl}). The former determines the *c*-axis penetration depth while the latter determines U_0. Van der Marel and Tsvetkov[12] proposed a phenomenological model of the dielectric response of such a superlattice of interbilayer and intrabilayer Josephson junctions. They showed that it exhibits a transverse resonance between the two zero crossings corresponding to the two plasmons. It has been suggested[13] that this new excitation (''transverse plasma excitation''), which can be visualized as a resonant oscillation of the condensate density between the two closely spaced copper-oxygen planes, has indeed been observed as an additional absorption peak that appears at low temperature in the spectra of the infrared *c*-axis conductivity of underdoped Y123.[14–17] Very recently, this interpretation has been put on a firm basis by a detailed analysis of the *c*-axis conductivity data for Y123 with different oxygen concentrations.[18,19] Note that the observation of the transverse plasma excitation also implies the existence of the second (intrabilayer) Josephson plasmon that is a vital ingredient of the ILT theory. This opens a possibility to test also for bilayer compounds the relationship between the Josephson coupling energy and the condensation energy predicted by the ILT theory [Eq. (1)].

In this paper we review some of the previous experimental observations of the transverse plasma excitation (TPE). In addition, new data for almost optimally doped Bi-2212 with

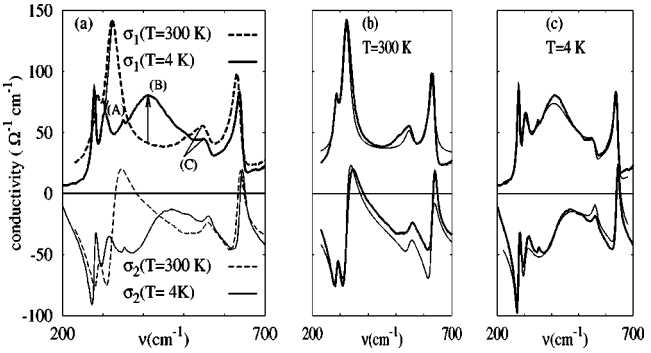

FIG. 1. (a) Experimental spectra of the *c*-axis conductivity, $\sigma = \sigma_1 + i\sigma_2$, of Y123 with $T_c = 53$ K. Experimental data (thick solid lines) and fits (thin solid lines) for (b) $T = 300$ K and (c) $T = 4$ K. The symbols (A), (B), and (C) indicate the most pronounced anomalies as discussed in the text. A slightly modified version of Fig. 1 from Ref. 30.

$T_c \approx 91$ K are reported and analyzed (Sec. II). In Sec. III, the Josephson coupling energies of different bilayer compounds obtained from the *c*-axis conductivity data of Refs. 18–21 and of the present work are compared with the condensation energies obtained from the specific-heat data.[22,23] Section IV contains a discussion of the frequently used sum-rules-based estimates of the changes of the *c*-axis kinetic energy.[24–26] Finally, an extension of the interlayer tunneling theory is proposed in Sec. V, which allows one to explain the high values of T_c in the single-layer compounds Tl-2201 and Hg-1201.

II. RESULTS AND DISCUSSION

Since the early days of the high-temperature superconductivity, it was known that some of the infrared-active *c*-axis phonon modes of the cuprate superconductors exhibit changes (so-called ''phonon anomalies'') in the vicinity of the superconducting transition temperature (see, e.g., Refs. 27–29). The most pronounced anomalies have been observed for underdoped Y123.[15–18]

A. $YBa_2Cu_3O_{7-\delta}$

The anomalies are illustrated in Fig. 1, which shows our experimental spectra of the *c*-axis conductivity of $YBa_2Cu_3O_{6.55}$ with $T_c = 53$ K.[18] Note the following anomalies. (A) As the temperature decreases, the oxygen-bond-bending mode at 320 cm^{-1} that involves the in-phase vibration of the planar oxygens against the Y-ion and the chain ions[31–33] loses most of its spectral weight and softens by almost 20 cm^{-1}; (B) at the same time a new broad absorption peak appears in the spectra around 410 cm^{-1}; (C) the spectral weight of the peak corresponding to the apical oxygen mode at 560 cm^{-1} decreases. The additional absorption peak [feature (B)] has been sometimes considered to be a new phonon.[15] On the other hand, van der Marel and coworkers suggested[13] that it corresponds to the TPE of their model.[12] We believe that this interpretation is correct, but one has to keep in mind that some part of the spectral weight of the peak ($\sim 50\%$) indeed comes from the phonons (see Ref. 17 for a detailed discussion). With increasing doping the additional peak shifts toward higher frequencies and it becomes broader and less pronounced.[18,17] Although the anomalies start to develop above T_c in strongly underdoped compounds, the pronounced and steep changes always occur right at T_c.[17] Similar though less spectacular effects have also been observed for other values of δ,[14–19,34] for several other bilayer compounds,[35–39] and for the trilayer compound $Tl_2Ba_2Ca_2Cu_3O_{10}$.[40] Also shown in Fig. 1 are the fits obtained using the model of Ref. 18. Since we are going to refer to this model rather frequently, we summarize its main ideas in the Appendix A. It can be seen that the model is capable of providing a good fit of both the normal and the superconducting state data. The same values of the oscillator strengths of the phonons have been used for the normal and for the superconducting states. This means that the changes of the spectral weight are accounted for by the model rather than simply fitted.

B. $Bi_2Sr_2CaCu_2O_8$

Very recently, Ž*elezný et al.*[20,21] have reported similar anomalies in the infrared *c*-axis conductivity of underdoped Bi-2212. The spectra exhibit an increase of the electronic background around 450 cm^{-1} below T_c accompanied by characteristic phonon anomalies. The increase of the background corresponds to the additional absorption peak such as observed in the spectra of underdoped Y123. The most pronounced phonon anomaly again consists in a sizable decrease of the spectral weight of the 355 cm^{-1} phonon mode, which has—according to the shell model calculations[41]—a similar eigenvector as the 320 cm^{-1} mode in Y123. The doping and temperature dependence of the anomalies is close to that observed in Y123. These findings of Ž*elezný et al.* confirmed that the anomalies are a common property of the bilayer cuprate compounds.

Figure 2 shows our experimental spectra of the *c*-axis optical conductivity of an almost optimally doped Bi-2212 single crystal with $T_c = 91$ K that have been obtained by ellipsometric measurements (see Ref. 17 and references therein for a description of the technique). The measurements have been performed on a large ac-face of size 4×0.5 mm^2. As shown in Fig. 2(b) the spectra exhibit the same kind of anomalies as underdoped Y123 (Refs. 14–18) and underdoped Bi-2212.[20,21] Below T_c the electronic background increases in the frequency region around 550 cm^{-1} [feature (B)] and simultaneously some of the infrared-active phonon modes are renormalized; in particular, the phonon mode at 355 cm^{-1} loses a large part of its spectral weight [feature (A)]. As compared to the data for underdoped Bi-2212, the region of the spectral weight increase is shifted toward slightly higher frequencies. This can be expected because the frequency of the TPE is known to increase with increasing hole doping (see Ref. 18 for a discussion). The onset temperature of the anomalies coincides with T_c [cf. the insets of Fig. 2(a) and Fig. 2(b)] which confirms that they are

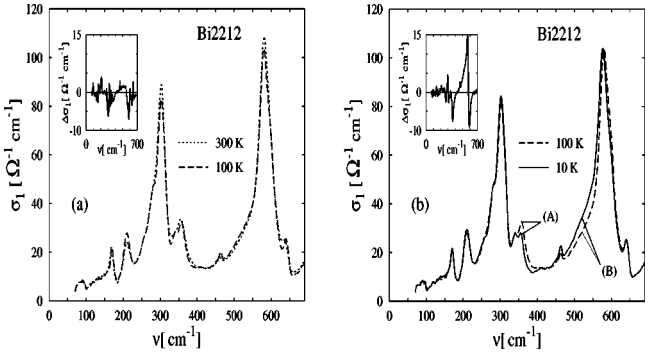

FIG. 2. Experimental spectra of the *c*-axis conductivity of almost optimally doped Bi-2212 with $T_c=91$ K. (a) Data for $T=300$ K and $T=100$ K. (b) Data for $T=100$ K and $T=10$ K. The insets of (a) and (b) display the differences $\sigma_1(T=100\ \mathrm{K})-\sigma_1(T=300\ \mathrm{K})$ and $\sigma_1(T=10\ \mathrm{K})-\sigma_1(T=100\ \mathrm{K})$, respectively. Note that the former and the latter difference correspond to a temperature change of 200 K and 90 K, respectively. The symbols (A) and (B) in (b) indicate the most pronounced anomalies as discussed in the text.

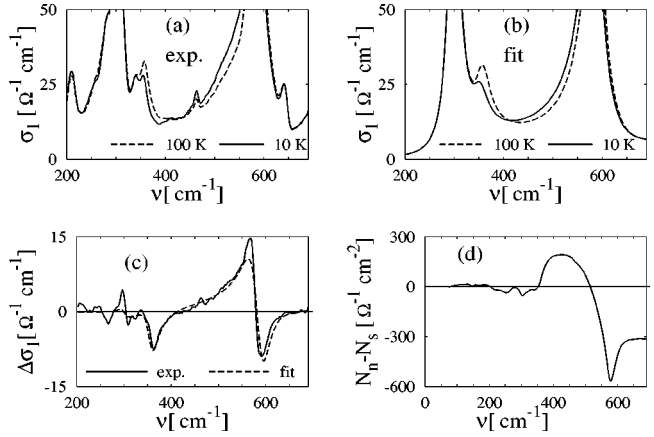

FIG. 3. (a) Experimental spectra of the *c*-axis conductivity of optimally doped Bi-2212-region of the spectra near the anomalies on an enlarged scale. (b) Fits of the spectra obtained by using the model of Ref. 18 as described in the text. (c) Spectra of $\sigma_1(T=100\ \mathrm{K})-\sigma_1(T=10\ \mathrm{K})$. (d) Spectra of the quantity N_n-N_s defined in the text.

related to superconductivity. Note that some signatures of the anomalies can also be found in the reflectivity data of Ref. 42.

Figure 3(a) displays the region near the anomalies on an enlarged scale and Fig. 3(b) shows the fits obtained by using a slightly modified version[21] of the model of Ref. 18. The modification concerns only the description of the featureless electronic background. First, the interbilayer susceptibility is set equal to zero ($\chi_{int}=0$ in notation of Ref. 18). This is a reasonable approximation considering the very low value of the unscreened interbilayer plasma frequency ω_{int} ($\omega_{int}\leqslant 20\ \mathrm{cm}^{-1}$, see Ref. 43). Second, the regular part of the intrabilayer susceptibility (χ_{bl}) has been fitted by a combination of a broad Drude term and a broad mid-infrared Lorentz oscillator instead of the single very broad Lorentzian centered at high frequencies that was used previously. Furthermore, we have adopted the simple picture of the phonon eigenvectors used in the fits of the spectra of underdoped Y123 and underdoped Bi-2212, i.e., we assume that the 355 cm^{-1} mode corresponds to the vibrations of the planar oxygens, whereas the modes at 300 cm^{-1} and 580 cm^{-1} correspond to vibrations of the interbilayer oxygens, i.e., the apical oxygens and the oxygens of the BiO layers. The values of the fitting parameters and other numerical factors used are summarized in Table I. Those corresponding to the room-temperature spectrum have been obtained by fitting the measured frequency dependence of the complex dielectric function in the frequency region above 300 cm^{-1} (with $\omega_{bl}=0$ and $S_{bl}=0$, S_{bl} being the oscillator strength of the mid-infrared Lorentz oscillator). Those used in calculating the 100−K spectrum have also been obtained by fitting the data (with $\omega_{bl}=0$ and $S_{bl}=0$), except for the values of ε_∞, S_P, S_1, S_2 (oscillator strengths of the phonons), ω_P (frequency of the oxygen-bond-bending mode), ω_1 (frequency of the 300 cm^{-1} mode), which have been fixed at the room-temperature ones. Finally, the values of ε_∞, S_P, S_1, S_2, ω_P, γ_P, ω_1, and γ_{bl} (broadening parameter of the broad Drude contribution), have been fixed at the 100 K ones, when fitting the low-temperature spectrum. It can be seen that the most pronounced features of the experimental spectra, in particular the increase of the electronic background around 550 cm^{-1} and the spectral-weight anomaly of the oxygen bond-bending mode, are well reproduced.

TABLE I. Values of the fitting parameters and other numerical factors used in fitting the measured *c*-axis infrared conductivity of optimally doped Bi-2212. The plasma frequency and the broadening parameter of the broad Drude peak are denoted by Ω_{bl} and γ_{bl}, respectively. The meaning of the other symbols is the same as in Ref. 18. The temperatures are given in K, the frequencies and the broadening parameters in cm^{-1}. The values of the numerical factors α, β, γ,[18] $\alpha=2.28$, $\beta=0.64$, $\gamma=1.28$ have been obtained in the same way as in Ref. 18 (see also Ref. 44) using the following values of the effective ionic charges: $e^*_{Bi}=3$, $e^*_{Sr}=2$, $e^*_{Ca}=2$, $e^*_{Cu}=2$, $e^*_O=-2$. The distances between the planes of a bilayer and between the neighboring bilayers are $d_{bl}=3.37$ Å and $d_{int}=12.03$ Å, respectively.

T	ε_∞	ω_{bl}	Ω_{bl}	γ_{bl}	S_{bl}	ω_b	γ_b	S_P	S_1	S_2	ω_P	ω_1	ω_2	γ_P	γ_1	γ_2
300	3.8	0	3000	1220	0	0	0	1.05	0.24	0.50	455	332	639	10	36	31
100	3.8	0	3000	1300	0	0	0	1.05	0.24	0.50	455	332	638	12	35	33
10	3.8	1180	2520	1300	2.04	1000	900	1.05	0.24	0.50	455	332	636	12	34	36

TABLE II. Values of the intrabilayer plasma frequency ω_{bl}, the Josephson coupling energy E_J and the condensation energy U_0 for several bilayer compounds. The values of ω_{bl} are taken from Ref. 18 (underdoped Y123), Ref. 19 (optimally doped Y123), and Ref. 21 (underdoped Bi-2212); the value for optimum doped Bi-2212 has been obtained as described in the text. The values of the condensation energies are taken from Ref. 22 (Y123) and Ref. 23 (Bi-2212).

Compound	T_c (K)	ω_{bl} (cm^{-1})	E_J (meV)	$U(0)$ (meV)	$E_J/U(0)$
$YBa_2Cu_3O_{6.45}$	25	950	0.08	0.01	8.0
$YBa_2Cu_3O_{6.55}$	53	1200	0.13	0.05	2.6
$YBa_2Cu_3O_{6.75}$	80	1780	0.30	0.16	1.8
$YBa_2Cu_3O_{6.93}$	91	3480	1.14	0.36	3.2
$Bi_2Sr_2CaCu_2O_8$	60	620	0.035	0.02	1.5
$Bi_2Sr_2CaCu_2O_8$	80	970	0.085	0.06	1.4
$Bi_2Sr_2CaCu_2O_8$	91	1180	0.13	0.13	1.0

Figure 3(c) shows the frequency dependence of the difference $\sigma_1(T=10\ \mathrm{K} \ll T_c) - \sigma_1(T=100\ \mathrm{K} \approx T_c)$. The value of the difference is positive in the frequency region between 420 cm^{-1} and 580 cm^{-1}, whereas it is negative both for lower frequencies (in the region between 340 cm^{-1} and 420 cm^{-1}) and for higher frequencies (in the region between 580 cm^{-1} and 650 cm^{-1}). The positive values in the first region are caused mainly by the increase of the electronic background below T_c (i.e., the additional peak due to the TPE). The negative values in the second region correspond to the spectral weight anomaly of the oxygen-bond-bending mode. The negative values in the third region are mainly due to a slight shift of the apical-oxygen mode at 580 cm^{-1} toward lower frequencies. The agreement between the difference of the measured data (full line) and the difference of the fitted spectra (dashed line) is excellent. Note, that this agreement has not been achieved by changing the values of the parameters of the phonon modes. The slight shift of the 580 cm^{-1} mode accounts only for a part of the spectral weight increase around 550 cm^{-1}.

Finally, the frequency dependence of the quantity $N_n - N_s$, where $N_n(\omega) = N(T=100\ \mathrm{K} \approx T_c, \omega)$, $N_s(\omega) = N(T=10\ \mathrm{K} \ll T_c, \omega)$ and

$$N(T,\omega) = \int_{0^+}^{\omega} d\omega' \sigma_1(T,\omega'), \tag{2}$$

is displayed in Fig. 3(d). We take our low-frequency cutoff of 70 cm^{-1} as the lower limit of the integration in Eq. (2), but it is rather unlikely that below this frequency there is any considerable difference between the normal state and the superconducting state data. For a conventional superconductor, the value of $N_n - N_s$ increases with increasing frequency and it approaches ρ_s, the spectral weight of the δ peak at $\omega = 0$, within a range of $\sim 6\Delta$, Δ being the superconducting gap.[45] It has been shown by Basov *et al.*[25] that for several high-temperature superconductors the value of $N_n - N_s$ also increases with increasing frequency but it saturates at a value of only about one half of ρ_s for $\omega \sim 10\Delta$. Our result for Bi-2212 exhibits an even more surprising tendency: $N_n - N_s$ stays approximately constant up to ~ 350 cm^{-1}, it changes considerably in the frequency region between 350 cm^{-1} and 620 cm^{-1} and it seems to saturate above ~ 650 cm^{-1} at a negative value of approximately $-300\ \Omega^{-1}\ cm^{-2}$. The corresponding value of the ratio $|N_n - N_s|/\rho_s$ is larger than 25. The fact that the value of $N_n - N_s$ above ~ 550 cm^{-1} is negative signals an increase of the low frequency spectral weight below T_c that is caused by the formation of the peak due to the TPE. Note that such an increase cannot be easily explained by any conventional theory. We shall come back to this interesting issue in Sec. IV B.

III. JOSEPHSON COUPLING ENERGIES AND CONDENSATION ENERGIES

In Table II we summarize the values of the intrabilayer plasma frequency (ω_{bl}), the corresponding Josephson coupling energy per unit cell (E_J), and the condensation energy per unit cell (U_0) for Y123 and Bi-2212. The values of E_J have been calculated using the formula[46]

$$E_J = \frac{\hbar^2 \varepsilon_0 a^2}{4e^2 d_{bl}} \omega_{bl}^2 \quad \text{or equivalently}$$

$$E_J\ [\mathrm{meV}] = \frac{C}{d_{bl}\ [\text{Å}]} (\omega_{bl}\ [\mathrm{cm}^{-1}])^2. \tag{3}$$

Here a is the in-plane lattice constant, d_{bl} is the distance between the closely spaced copper-oxygen planes, and $C = 3.1 \times 10^{-7}$. We neglect the contribution of the interbilayer plasmon to E_J that is by at least one order of magnitude lower than that of the intrabilayer one. Note that Eq. (3) does not contain any adjustable parameters. The values of the condensation energies have been obtained from the specific-heat data in Ref. 22 (Y123) and in Ref. 23 (Bi-2212). We estimate the error bars of the values of ω_{bl} to be about 20 $-30\,\%$. These error bars arise mainly from the uncertainty in the description of the electronic background.[47] The corresponding uncertainties of the values of E_J are about 50%. Taking this into account, the agreement between the Josephson coupling energies obtained from the optical data and the condensation energies obtained from the specific-heat data is reasonably good as described in the following.

(i) The values of the two quantities are of the same order of magnitude.

(ii) Both quantities exhibit a rather similar dependence on doping. It is even possible to understand, why the values of the ratio E_J/U_0 are higher for the strongly underdoped samples than for the less underdoped ones or the optimally doped ones. It is, namely, likely that for strongly underdoped samples some fluctuation effects set in well above the macroscopic transition temperature T_c. This suggestion is consistent with the finding that the phonon anomalies start to occur well above T_c in strongly underdoped samples.[17,18,48] The contribution of the fluctuation effects to the condensation energy is not likely to be contained in the values of U_0 presented in Table II, since they have been obtained by an analysis of the specific-heat data where only the changes occurring below T_c are properly taken into account. On the other hand, the values of E_J do contain the contribution of these effects, since they are determined by the low-temperature values of ω_{bl} (i.e., in a way that does not require any assumptions concerning the onset of superconductivity). As a result the values of U_0 for strongly underdoped samples can be expected to be smaller than the values of E_J.

(iii) The values of E_J for Y123 are systematically higher than those for Bi-2212, in agreement with the trend in the condensation energies. It may be argued that the difference in the condensation energies is related to the presence of metallic chains in Y123. However, the chain condensation cannot fully account for the difference, since Ca-substituted samples with broken chains also have a significantly higher condensation energy than Bi-2212.[22]

This agreement means that the values of the condensation energies of the bilayer compounds can be explained using the ILT theory. Further implications will be discussed in Sec. V. It certainly remains an open question why different compounds with almost identical values of T_c have rather different values of the condensation energy.

IV. SUM RULES

There is another approach to estimate the changes of the *c*-axis kinetic energy, pioneered by Chakravarty[4] and Chakravarty, Kee, and Abrahams,[24] which is based on the use of the optical sum rule. For the bilayer compounds, this approach yields an opposite result, namely, that the value of the condensation energy cannot be accounted for by the change of the *c*-axis kinetic energy. In the first part of this section we clarify several conceptual points that have made the discussions of the kinetic energy changes somewhat confusing (Sec. IV A). Next we discuss some specific properties of the bilayer compounds (Sec. IV B). In particular, we show that for these compounds the change of the *c*-axis kinetic energy cannot be estimated using the conventional ''tight-binding'' sum rule of Refs. 4 and 24.

A. Conceptual issues

For simplicity, we focus in our considerations first on the single-layer compounds. In the present context, there are at least three different quantities denoted as *c*-axis kinetic energy. First, the ''true'' *c*-axis kinetic energy, $K_c = \Sigma_i p_{i,c}^2/2m$. Second, the ''tight-binding'' *c*-axis kinetic energy H_c,

$$H_c = -\sum_{l,i,j,s} t_\perp(l,i,j) c^+_{j,l+1,s} c_{i,l,s} + \text{H.c.}, \tag{4}$$

where l is the layer index, *i* and *j* refer to the sites of the two-dimensional layers, *s* refers to spin, $t_\perp$ is the interlayer hopping matrix element, and H.c. means the Hermitian conjugate operator. Third, the effective low-energy *c*-axis kinetic energy of the ILT theory H_J,

$$H_J = -\sum_{l,\mathbf{k}} T_J(\mathbf{k}) c^+_{\mathbf{k},l+1,\uparrow} c^+_{-\mathbf{k},l+1,\downarrow} c_{-\mathbf{k},l,\downarrow} c_{\mathbf{k},l,\uparrow} + \text{H.c.}, \tag{5}$$

i.e., the Josephson coupling energy. The experimental data are discussed in terms of at least two different sum rules. First, the ''general'' sum rule (for derivation see, e.g, Ref. 49),

$$\int_0^\infty \sigma_1(T,\omega)\, d\omega = \frac{\pi n e^2}{2m}, \tag{6}$$

which is fulfilled for any real system and second, the ''tight-binding'' sum rule valid only for model Hamiltonians whose single-particle part is of the tight-binding form (for derivation see, e.g., Refs. 50,4 and references therein),

$$\int_0^\infty \sigma_1(T,\omega)\, d\omega = -\frac{\pi e^2 d}{2\hbar^2 a^2} \langle H_c \rangle (T). \tag{7}$$

In Eq. (6), *n* is the total electron density, in Eq. (7) *a* is the in-plane lattice constant, *d* is the lattice constant along the *c* axis, and H_c is the tight-binding kinetic energy [Eq. (4)] per unit cell ($\langle H_c \rangle$ represents an average of this quantity, *T* is the temperature).

Let us discuss possible changes of the three kinetic energies upon entering the superconducting state and the relations between them and the sum rules.

(i) There is no obvious relation between $\langle K_c \rangle$ and the sum rules. Upon entering the superconducting state, the total energy of the superconductor decreases. This implies—by virtue of the virial theorem ($\langle K \rangle = -\langle V \rangle/2$, where *K* and *V* are the kinetic and the potential energy, respectively; see, e.g., Ref. 51)—that its total kinetic energy increases. It is possible to assume that even $\langle K_c \rangle$ increases at the superconducting transition.

(ii) It is very likely that the degrees of freedom essential for superconductivity are contained in some model single-band Hamiltonian H_{1b} whose (tight-binding-like) single-particle part is derived by a downfolding process in which all of the higher-energy bands are integrated out[52] and whose interaction part describes the most pronounced correlation effects. In our opinion, there are no general reasons why the average of its *c*-axis kinetic energy term H_c [Eq. (4)] should decrease or increase below T_c. The arguments invoking a frustration of the *c*-axis kinetic energy in the normal state and a ''deconfinement'' of bosonic pairs below T_c (See, e.g.,

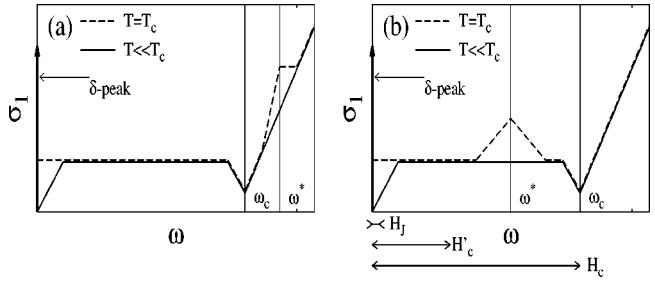

FIG. 4. Schematic representation of the spectral-weight changes upon entering the superconducting state. The increase of spectral weight at low frequencies below T_c is compensated by a decrease around some frequency ω^*. This frequency may be either (a) higher or (b) lower than the interband cutoff ω_c. The horizontal lines below the frequency axis of (b) indicate the three frequency scales corresponding to the three effective *c*-axis kinetic energies discussed in the text.

Ref. 2, Chapter 2, Dogma VI, and Ref. 3) are usually based on asymptotic properties of the quasiparticle propagators, i.e., they concern rather the asymptotic behavior for $\omega \rightarrow 0$ than the actual changes of $\langle H_c \rangle$. Possibly these arguments could be formulated more precisely in terms of yet another effective kinetic energy H_c' characterizing the *c*-axis electrodynamics in a frequency scale intermediate between that of H_c ($\sim 10\,000$ cm^{-1}) and the frequency scale of H_J of the order of 100 cm^{-1} (Ref. 53) (see Fig. 4).

It follows from Eq. (7) that the possible change of $\langle H_c \rangle$ at the superconducting transition is related to the change of the spectral weight as follows:

$$[\langle H_c \rangle_s (T \ll T_c) - \langle H_c \rangle_n (T \approx T_c)]\,[\mathrm{meV}] = -\frac{4C}{d\,[\text{Å}]}\,\frac{120}{\pi}\left(\int_0^{\Omega_c} \sigma_1(T \ll T_c, \omega)\, d\omega - \int_0^{\Omega_c} \sigma_1(T \approx T_c, \omega)\, d\omega \right) [\Omega^{-1}\ \mathrm{cm}^{-2}], \quad (8)$$

where Ω_c is a cutoff frequency required to exhaust the sum rule (7). Note that in a model involving strong correlations, the value of Ω_c may be much higher than the bandwidth of the corresponding noninteracting model. In addition, this value (and also the changes of the kinetic energy themselves) may depend on the kind of model that is used, i.e., on the interaction part of the model Hamiltonian H_{1b}.

(iii) We emphasize that it is the effective *c*-axis kinetic energy H_J of the ILT theory [Eq. (5)] whose changes at the superconducting transition were predicted to be responsible for the high values of T_c in Ref. 1. The only ''sum rule,'' which can be associated with H_J, is Eq. (3) with d_{bl} substituted by d (note that $E_J = -\langle H_J \rangle$).

What is the experimental status? The analysis of Basov *et al.*[25] demonstrates that at least for the underdoped high-T_c superconductors, the low-frequency spectral weight

$$\alpha(T,\omega) = \int_0^{\omega} \sigma_1(T,\omega')\, d\omega' = \rho_s(T) + N(T,\omega) \quad (9)$$

increases considerably upon entering the superconducting state for cutoff frequencies ω ranging up to at least 1200 cm^{-1}. More precisely, as one increases the value of ω, the value of the difference $\alpha(T \ll T_c, \omega) - \alpha(T \approx T_c, \omega)$ saturates at $\omega \approx 500$ cm^{-1}, reaching typically 50% of ρ_s. The only way to reconcile this interesting finding with the general sum rule (6) consists in assuming[25] that a substantial part of $\alpha(T \ll T_c, 1200\ \mathrm{cm}^{-1})$ is collected from frequencies exceeding 1200 cm^{-1}. In other words, since the total spectral weight has to be conserved, the increase of $\alpha(T, 1200\ \mathrm{cm}^{-1})$ below T_c is compensated by a decrease of spectral weight around some frequency ω^* higher than 1200 cm^{-1}. A sketch of the situation is shown in Fig. 4.

What do we learn from these results about the changes of the tight-binding kinetic energy $\langle H_c \rangle$? Let us denote by ω_c the interband cutoff, i.e., the upper limit of the frequency interval for which the response of the superconductor can be properly described using a certain effective Hamiltonian H_{1b} (e.g., the Hubbard Hamiltonian). Let us further assume, for the sake of simplicity, that $\omega_c \geqslant \Omega_c$ of Eq. (8).[54] There are two different possibilities, which are both compatible with the infrared data: (a) $\omega^* > \omega_c$ and (b) $\omega^* < \omega_c$ (see Fig. 4). In case (a), it follows from Eqs. (6) and (8) that $\langle H_c \rangle$ indeed decreases below T_c. In order to establish this decrease experimentally, however, one would have to estimate the total low-frequency spectral weight above and below T_c, i.e., to integrate $\sigma_1(\omega)$ up to ω_c. We believe that the case (b) is more likely to happen. The increase of $\alpha(T, 1200\ \mathrm{cm}^{-1})$ below T_c and the corresponding decrease of the spectral weight around ω^* then both can be described by using H_{1b}. It follows from Eqs. (6) and (8) that $\langle H_c \rangle$ does not change at T_c. To conclude, it is only the tight-binding *c*-axis kinetic energy H_c [Eq. (4)] of an effective single-band Hamiltonian, whose change at the superconducting transition can be obtained using Eq. (8). The results of Basov *et al.*[25] nicely reveal the unconventional properties of the high-temperature superconductors, in particular the extremely large frequency scale involved, but they cannot be used to yield reliable estimates of this change because of the uncertainties concerning the cutoff frequencies Ω_c and ω_c. In addition, there are no *a priori* reasons, why $\langle H_c \rangle$ should change upon entering the superconducting state.

Another example of a model *c*-axis kinetic energy is represented by the effective low-energy *c*-axis kinetic energy H_J [Eq. (5)] of Ref. 1. It acquires a nonzero (negative) value, $-E_J$ [Eq. (3)], only in the superconducting state and it was predicted to be responsible for the high values of T_c. It is certainly a crude approximation to identify E_J with the *c*-axis contribution to the condensation energy, as we did it in the previous section, since possible ''countereffects''[55] are not included. They are to some extent included when estimating the changes of the *c*-axis kinetic energy using Eq. (8) with the upper limit of the integrals well below ω^* (instead of ω_c), i.e.,

$$\Delta E_{kin,c}\ [\mathrm{meV}] = -\frac{4C}{d[\text{Å}]}\,\frac{120}{\pi}[\alpha(T \ll T_c, \omega < \omega^*) - \alpha(T \approx T_c, \omega < \omega^*)]\,[\Omega^{-1}\ \mathrm{cm}^{-2}]. \quad (10)$$

This is an appealing possibility, but the physical meaning of the result is not completely clear (in contrast to the change of the well-defined quantity $\langle H_c \rangle$). It may be perhaps viewed as an estimate of the change of some kinetic energy H_c' characterizing the *c*-axis electrodynamics in an intermediate frequency scale (see our discussion above and Fig. 4). Note finally that the fact that $\Delta E_{kin,c}$ includes the countereffects does not necessarily imply that $|\Delta E_{kin,c}| < E_J$ because of the additional factor of 4 entering the sum-rules-based formulas.[56] On the contrary, for moderate countereffects, $|\Delta E_{kin,c}| > E_J$. For underdoped $La_{2-x}Sr_xCuO_4$, e.g., $|\Delta E_{kin,c}|$ is by a factor of ~ 2 larger than E_J.[56]

B. Some specific properties of the bilayer compounds

In Fig. 3(d), we have encountered a rather unusual situation. First, the value of the quantity $N(T,\ 690\ \mathrm{cm}^{-1})$ defined by Eq. (2) increases with decreasing temperature. A phenomenon not observed for any of the single-layer compounds (see, e.g., Ref. 25). Second, the increase of the integrated spectral weight $\alpha(T,\ 690\ \mathrm{cm}^{-1})$ defined by Eq. (9) upon entering the superconducting state is lower by a factor of ~ 30 than the value required to yield a kinetic-energy change comparable to U_0 [when inserted into Eq. (10)). On the other hand, using simply the formula (3) for the Josephson coupling energy, we have obtained a value fairly close to U_0. Here we propose a qualitative explanation of these paradoxes.

Let us consider the superlattice of intrabilayer and interbilayer Josephson junctions. The low-frequency spectral weight $\alpha(T \ll T_c, \omega > \omega_p)$, where ω_p is the frequency of the TPE [Eq. (A2)], contains both the contribution of the δ peak at $\omega = 0$, S_δ [Eq. (A3)], and the contribution of the TPE at $\omega = \omega_p$, S_{pl} [Eq. (A4)]. The appearance of the second one below T_c explains the first paradox. It is easy to show that

$$\alpha(T \ll T_c, \omega > \omega_p) = \frac{\pi}{2}\varepsilon_0 \frac{d_{bl}\omega_{bl}^2 + d_{int}\omega_{int}^2}{d_{bl} + d_{int}} \approx \frac{\pi}{2}\varepsilon_0 \frac{d_{bl}\omega_{bl}^2}{d_{bl} + d_{int}}, \tag{11}$$

where d_{int} is the distance between the bilayers. The Josephson coupling energy is approximately given by Eq. (3) (neglecting the contribution of the interbilayer Josephson junction), whereas the change of the *c*-axis kinetic energy estimated using Eqs. (10) and (11) is given as follows:

$$\Delta E_{kin,c}\ [\mathrm{meV}] = -\frac{4C}{(d_{bl} + d_{int})\ [\text{Å}]} \frac{d_{bl}(\omega_{bl}\ [\mathrm{cm}^{-1}])^2}{d_{bl} + d_{int}}. \tag{12}$$

It can be seen that

$$E_J \gg |\Delta E_{kin,c}|. \tag{13}$$

This is the explanation of the second paradox. The effects of the electronic background make the discrepancy even more pronounced. At the same time, it is obvious that within the simple model of the superlattice of intrabilayer and interbilayer Josephson junctions, it is the Josephson coupling energy E_J, rather than $\Delta E_{kin,c}$, which represents the change of the *c*-axis kinetic energy upon entering the superconducting state. We conclude that for the bilayer compounds the change of the *c*-axis kinetic energy can be estimated using Eq. (3) but cannot be estimated using Eq. (10). We refer the reader to Appendix B for a more rigorous discussion.

V. POSSIBLE EXTENSION OF THE ILT SCENARIO FOR SINGLE LAYER COMPOUNDS

In Sec. III we have shown that for the bilayer cuprate compounds the Josephson coupling energy such as estimated from the optical data can account for the condensation energy. In Sec. IV B we have shown that this result is not invalidated by the fact that Eq. (10) yields a much lower estimate of the change of the *c*-axis kinetic energy upon entering the superconducting state than Eq. (3). The main reason of the discrepancy is that the tight-binding sum rule of Eq. (7) used to derive Eqs. (8) and (10) is only valid for such single-layer compounds, for which the distribution of the total electric field is homogeneous. The results presented in Sec. III thus suggest that the high-temperature superconductivity in the bilayer compounds can be accounted for by the ILT theory. We are left with three possible explanations.

(a) The agreement between the Josephson coupling energies and the condensation energies reported in Sec. III represents a mere coincidence.

(b) The interlayer tunneling indeed provides the dominant contribution to the condensation energy of the bilayer compounds. Another mechanism is responsible for the high values of T_c in the single-layer compounds Tl-2201 and Hg-1201.

(c) A modified ILT theory may explain the high-temperature superconductivity both in the bilayer compounds and in the single-layer compounds.

In our opinion, it is unlikely that case (a) is realized. It would mean either that the assignment of the additional absorption peak to the TPE (Refs. 13,18,19) is wrong or that the Josephson coupling energy is completely (or almost completely) compensated by the countereffects.[55] There are several important arguments supporting the present interpretation of the data. Let us mention two of them. First, the doping dependence. The frequency of the maximum of the additional absorption peak increases considerably with increasing doping. This is easy to explain within the present scenario (the squared frequency of the maximum should be proportional to the condensate density) but difficult to explain within theories where the additional peak is assigned to a pair-breaking excitation.[57,58] According to these theories the frequency of the maximum should be close to the pair-breaking frequency observed in other experiments, which seems not to be the case for strongly underdoped samples. One could argue[59] that the final-state interactions may shift the peak toward lower frequencies. Second, both the frequency and the spectral weight of the additional peak are determined by a single parameter ω_{bl}.[60] In other theories, at least two parameters are required to fit the data, e.g., Δ and $t_\perp$. Starting from our interpretation of the data, large countereffects would represent the only possibility to rule out the ILT mechanism from the role of the mechanism providing the dominant contribution to the condensation energy U_0.

Note that the values of the Josephson coupling energies presented in Table II are so high that even sizable countereffects of the order of 80% would not invalidate our interpretation (see Ref. 56). A possible analysis of the countereffects along the lines of Appendix B is complicated by the fact that the normal-state data for very low temperatures, which should be compared to the superconducting-state data rather than the data obtained for temperatures above T_c, are not available. If case (b) were realized, there would be two different mechanisms causing the high values of T_c. This is certainly not impossible. In the remaining part of this section we argue that even the possibility (c) should not be excluded. We propose an extension of the ILT theory, which may explain the high-T_c values in the single-layer compounds Tl-2201 and Hg-1201. For concreteness we focus on the Tl-2201 compound, for which some optical data are already available.[6,8,9,61,25,62]

According to the ILT theory as formulated, e.g., in Ref. 2, the *c*-axis kinetic energy is frustrated in the normal state because of the spin-charge separation mechanism. The electrons or holes are composite objects that cannot escape from the copper-oxygen planes (so-called ''confinement''). For Cooper pairs this confinement is relaxed and consequently the *c*-axis kinetic energy decreases at the superconducting transition. To our best knowledge, it has been previously always assumed that this decrease is related to the onset of Josephson tunneling between the superconducting copper-oxygen planes. This is, however, only one possible mechanism for the decrease. We suggest that in Tl-2201 the *c*-axis kinetic energy decreases via some delocalization of the Cooper pairs that involves the apical-oxygen orbitals. By the delocalization we mean the fact that the superconducting-state wave function acquires a larger contribution of the apical-oxygen orbitals than the normal-state wave function. Quite generally, the *c*-axis kinetic energy decreases at the superconducting transition, whenever the Cooper pairs are more delocalized along the *c*-axis than the single electrons or holes in the normal state. Note that our extension of the ILT theory is based on a radical form of the ''confinement'' hypothesis. Not only the hopping between the copper-oxygen planes is assumed to be blocked in the normal state but also (at least to some extent) the hopping between the orbitals of the copper-oxygen planes and the apical-oxygen orbitals. The conjecture can be experimentally tested in several ways. First we discuss the *c*-axis infrared spectra, which may already provide some evidence in favor of the proposed scenario. Next we briefly mention some other experimentally verifiable consequences.

Recently, some infrared data for Tl-2201 have been reported.[25,62] The spectra of the *c*-axis conductivity exhibit four peaks corresponding to the *c*-axis infrared phonons —instead of five as dictated by symmetry—and two other distinct features, which have not been discussed previously:

(i) A pronounced step around 210 cm^{-1}. For convenience, the relevant part of the conductivity spectra is shown in the inset of Fig. 5(b). Note that a weak feature at ~ 230 cm^{-1} in the grazing incidence reflectivity data of Ref. 61 may be related just to this step. We suggest that the step is due to the missing fifth *c*-axis infrared phonon.

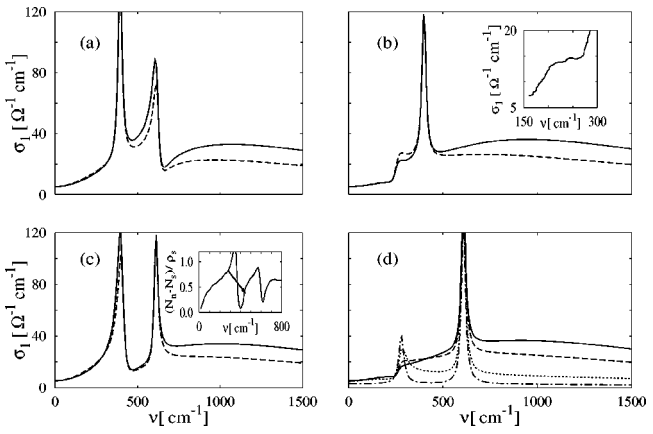

FIG. 5. Results of model computations of the *c*-axis infrared conductivity of Tl-2201. The results shown in (a) and (b) have been obtained using the assignment $A1$ (the Tl-layer oxygens vibrate at the highest frequency, the apical oxygens at ~ 400 cm^{-1}), those shown in (c) and (d) correspond to the reverse assignment ($A2$). The results shown in (a) and (c) have been obtained considering the region A as ''intrabilayer,'' those shown in (b) and (d) have been obtained considering the region A as ''interbilayer.'' The planar oxygen mode manifests itself as a step around 240 cm^{-1} in (b) and (d). The dashed and solid lines correspond to the two values of the plasma frequency of region A, Ω_{A1} and Ω_{A2}, $\Omega_{A1}<\Omega_{A2}$, respectively, as discussed in the text. The dotted and dashed-dotted lines in (d) represent results for $\Omega_A=1500$ cm^{-1} and $\Omega_A=600$ cm^{-1}, respectively. The inset of (b) displays the step in the experimental data of Ref. 25. The inset of (c) displays the experimental spectra of $(N_n-N_s)/\rho_s$ taken from Ref. 25. The arrow demonstrates the increase of the spectral weight of the phonon peak at 390 cm^{-1} in the superconducting state, as discussed in the text.

(ii) An increase of the spectral weight of the phonon peak at 390 cm^{-1} upon entering the superconducting state. It can be concluded from Fig. 3 of Ref. 25 that the spectral weight in the frequency region between 280 cm^{-1} and 440 cm^{-1} slightly (but not negligibly) increases below T_c. For convenience, the important part of the data is shown in the inset of Fig. 5(c). We estimate that the spectral weight increase represents 3–5 % of the spectral weight of the phonon.

Below we show that both features (i) and (ii) are compatible with the suggested extension of the ILT theory.

Figure 6 shows the crystal structure of Tl-2201 such as reported in Ref. 63. The simplest way to explore the possible consequences of our hypothesis consists in dividing the structure into regions A and B (denoted in Fig. 6), assuming that they exhibit different properties (region B being rather insulating and region A being more metallic), and applying the model of Ref. 18. In order to be able to apply the model, we have to make some assumptions concerning the eigenvectors of the phonons. Similarly as in case of Bi-2212 we concentrate on the three phonons located at higher frequencies (see Fig. 2 of Ref. 25) presumably corresponding to vibrations of the oxygens: the phonon mode at 600 cm^{-1}, the mode at 390 cm^{-1}, and the phonon that shows up as the step at 210 cm^{-1}. According to the shell model calculations of Ref. 64, the highest frequency mode involves vibrations of

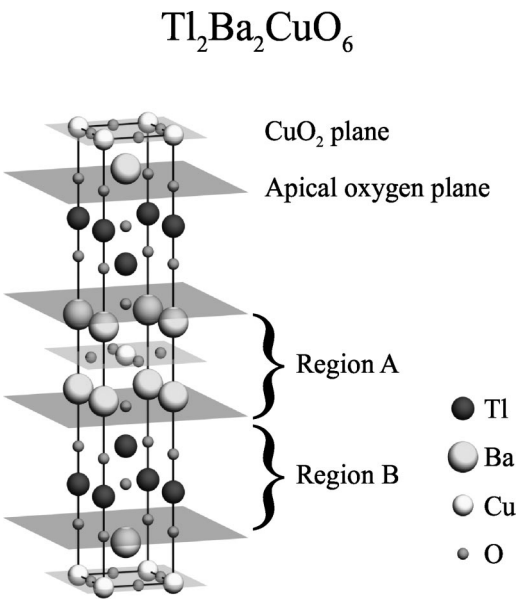

FIG. 6. Crystal structure of $Tl_2Ba_2CuO_6$.

the TlO-layer oxygens, the second one mainly vibrations of the apical oxygens, and the third one vibrations of the planar oxygens. Besides this assignment (*assignment A1*), we have also considered the possibility that the highest-frequency mode corresponds to vibrations of the apical oxygens (as in many other cuprates) and the second one to vibrations of the TlO-layer oxygens (*assignment A2*). In reality the vibrations of the apicals and the TlO-layer oxygens are probably strongly coupled. Figure 5 shows the results of our simulations. Parts (a) and (b) have been obtained using the assignment $A1$, parts (c) and (d) using the assignment $A2$. The model in the form presented in Ref. 18 allows us to treat only two phonon modes at the same time (the ''interface'' one, i.e., the apical-oxygen mode, and only one of the other two modes). This is the reason why there are two figures for a given assignment, each showing only two structures related to the phonons. The electronic conductivities of the two regions A and B (σ_A and σ_B) have been modeled, for the sake of simplicity, by broad Drude terms, the plasma frequency of the region A, Ω_A, being much higher than the plasma frequency of the region B. The results are shown for two different values of Ω_A: Ω_{A1} (dashed line) and Ω_{A2} (solid line), $\Omega_{A1}<\Omega_{A2}$. The increase of Ω_A may simulate the changes brought about by the superconducting transition: the more delocalized the ground-state wave function, the more metallic the region A and the higher the value of Ω_A. For the sake of simplicity, we do not consider the changes of σ_B caused by the onset of superconductivity. The values of the parameters used are given in Table III.

It can be seen in Figs. 5(b) and 5(d) that the lowest-frequency mode manifests itself as a step rather than as a Lorentzian peak, in agreement with the experimental data. Note that the step is getting less pronounced with increasing value of Ω_A, i.e., with increasing metallicity of the region A. This may correlate with an apparent absence of the structure in the data for strongly overdoped Tl-2201 (see Fig. 2 of Ref. 62). As seen in Figs. 5(a) and 5(c), the phonon mode involving vibrations of the TlO-layer oxygens exhibits distinct changes with increasing value of Ω_A, in particular its spectral weight increases.[65] This may correspond to the observed spectral weight anomaly of the 390 cm^{-1} phonon mode (assuming that the assignment $A2$ is closer to reality than the assignment $A1$). Finally, the increase of Ω_A results in an increase of the electronic background around 1000 cm^{-1} (concerning the absolute values, see Ref. 66). Such an increase should be observed in future experiments. Note that in the present simulations, the increase of Ω_A is intentionally relatively high so that the anomalies are clearly seen. Such an increase would correspond to a change of the *c*-axis kinetic energy much higher [by a factor of ~ 4, a rough estimate obtained by using Eq. (B11)] than the condensation energy.[67] The actual changes of the electronic background to be observed experimentally therefore should be considerably smaller (e.g., by a factor of 4). Also the frequency range of the increase may be somewhat different. To summarize, our simulations demonstrate that the anomalous features (i) and (ii) can be explained within a model involving the variations of the electric field inside the unit cell, whereas they cannot be easily explained in a conventional way. The important point is that if the electric field indeed changes considerably inside the unit cell, the changes of the *c*-axis kinetic energy upon entering the superconducting state cannot be estimated simply from the value of the plasma frequency of the superconducting condensate or by using the modified tight-binding sum rule (10).

Let us compare the *c*-axis conductivity of Tl-2201 with that of another single layer compound with considerably lower T_c, $Bi_2Sr_2CuO_6$ (Bi-2201). The spectra for Bi-2201 exhibit five peaks corresponding to the *c*-axis infrared phonons (See Fig. 2 of Ref. 61, similar results have been obtained by our group[68]), i.e., there is one phonon peak more than in the spectra for Tl-2201. This difference finds a natu-

TABLE III. Values of the parameters and other numerical factors used in modeling the *c*-axis infrared conductivity of Tl-2201. The plasma frequency and the broadening parameter of σ_A and σ_B are denoted by Ω_A and γ_A, and Ω_B and γ_B, respectively. The parameters of the phonons are denoted by S_1, ω_1, γ_1, S_2, ω_2, γ_2, S_3, ω_3, γ_3. The frequencies and the broadening parameters are given in cm^{-1}. The values of the numerical factors α, β, γ have been obtained in the same way as in Ref. 18 (see also Ref. 44) using the following values of the effective ionic charges: $e^*_{Tl}=3$, $e^*_{Ba}=2$, $e^*_{Cu}=2$, $e^*_O=-2$. The distances between the apical-oxygen planes are $d_A=5.3$ Å and $d_B=6.3$ Å, respectively.

ε_∞	Ω_{A1}	Ω_{A2}	γ_A	Ω_B	γ_B	S_1	S_2	S_3	ω_1	ω_2	ω_3	γ_1	γ_2	γ_3
5	2500	3000	2000	600	2000	0.6	0.5	0.5	300	440	640	25	20	25

ral explanation within our extension of the ILT theory. Bi-2201 has a substantially lower condensation energy than Tl-2201.[69,70] This suggests that in Bi-2201 the apical-oxygen orbitals are less accessible for the charge carriers. Consequently, the region A is much less metallic than in case of Tl-2201 and the planar-oxygen mode manifests itself rather as a peak than as a step feature. This is demonstrated in Fig. 5(d), where the results for $\Omega_A = 1500$ cm^{-1} (dotted line) and $\Omega_A = 600$ cm^{-1} (dashed-dotted line) are shown.

An observation of the infrared anomalies discussed above in more precise future experiments would represent a clear but indirect evidence in favor of the suggested extension of the ILT theory. Direct evidence could be provided by experiments probing the occupation of individual atomic orbitals, as, e.g., the near-x-ray absorption fine structure (NEXAFS) measurements (see, e.g., Ref. 71). We predict that such experiments will reveal a sizable increase of the number of holes on the apical sites at T_c accompanied by the corresponding decrease of the number of holes in the copper-oxygen planes. Note that this prediction does not concern only Tl-2201 but all the single-layer high-T_c cuprates. It may, of course, also be fulfilled for some of the bilayer cuprates. The changes of the hole distribution at T_c should further result in some structural changes, in particular, in changes of the distance between the apical oxygens and the copper-oxygen planes, and in anomalies of some Raman-active phonon modes involving vibrations of the apical oxygens. Such anomalies may already have been observed.[72]

VI. SUMMARY

The *c*-axis infrared conductivity of optimally doped Bi-2212 exhibits the same kind of anomalies as that of underdoped Y123. Below T_c the electronic background increases in the frequency region around 550 cm^{-1} and at the same time the oxygen-bond-bending mode at 355 cm^{-1} loses a large part of its spectral weight. The anomalies can be explained within a model involving the intrabilayer Josephson effect and variations of the electric field inside the unit cell. We have compared the Josephson coupling energies of Y123 and Bi-2212 with different oxygen concentrations obtained from the optical data with the condensation energies obtained from the specific-heat data and we have found that there is a remarkable agreement between the values of the two quantities. The Josephson coupling energy is shown to represent a reasonable estimate of the change of the *c*-axis kinetic energy upon entering the superconducting state and it is also shown that the latter quantity cannot be obtained by using the simple ''tight-binding'' sum rule, since this sum rule has been derived assuming homogeneous distribution of the total electric field within the unit cell. The most plausible interpretation of the agreement between the Josephson coupling energies and the condensation energies is that the condensation energy of the bilayer compounds can be accounted for by the interlayer tunneling theory. We propose a modification of this theory that may also explain the high values of T_c in Tl-2201 and Hg-1201. The main idea is that the *c*-axis kinetic energy of these compounds decreases at T_c via a delocalization of the Cooper pairs onto the apical-oxygen orbitals. We have investigated, using a toy model, the consequences of this hypothesis for the *c*-axis infrared response and we have demonstrated that it offers a simple explanation of two features observed in the measured *c*-axis conductivity of Tl-2201. In addition, we propose that for Tl-2201 an increase of the electronic backround around 1000 cm^{-1} takes place at T_c. We further predict a sizable increase at T_c of the number of holes on the apical sites, related structural changes and related anomalies of some Raman-active phonon modes.

Note added. There are some similarities between our model[18] of the charge dynamics and the models of Refs. 73–77. In Ref. 75 it is argued that the role of the intrabilayer plasmon could be played by an antiphase oscillation between the copper-oxygen planes and the ordered blocking-layer plaques. After submitting the paper, O. K. Andersen has drawn our attention to a preprint of Pavarini *et al.*,[78] where it is shown that there is a correlation between the maximum value of T_c for a given compound, $T_{c\,max}$, and the value of the parameter r that expresses the range of the intralayer hopping, t'/t, obtained from band structure calculations. The higher the value of r, the higher the value of $T_{c\,max}$. It remains an open question to what extent this correlation is consistent with the extension of the ILT theory proposed in Sec. V. There we have suggested that the condensation energy of the single-layer compounds is largely due to a change of the *c*-axis kinetic energy at T_c connected with an increase of the number of holes on the apical sites. The reason for this change is the confinement of the holes to the copper-oxygen planes in the normal state and a deconfinement of the Cooper pairs below T_c. In case of the single-layer systems the condensation energy—and also T_c—thus should be the largest (ignoring the material dependence of the orbital energies) for the compounds with the largest value of the hopping matrix element t_{pa} between the relevant orbital of a copper-oxygen plane (predominantly $d_{x^2-y^2}$) and the $2p_z$ orbital of the neighboring apical-oxygen plane. The $2p_z$ orbital of an apical oxygen couples to the copper $4s$ orbital and t_{pa} is thus determined (a) by the matrix element t_{sc} between the $2p_z$ orbital and the Cu $4s$ orbital and (b) by the ratio of the Cu $4s$ to Cu $d_{x^2-y^2}$ character, R. The value of t_{sc} decreases[78] with increasing distance d between the copper-oxygen plane and the apical-oxygen plane and it is thus somewhat smaller for Tl-2201 ($d \approx 2.7$ Å) and Hg-1201 ($d \approx 2.8$ Å) as compared to $LaSrCuO_4$ ($d \approx 2.4$ Å). On the other hand, the value of R increases with increasing value of r as r^2,[78] which means that it is much larger for Tl-2201 ($r \approx 0.33$) and Hg-1201 ($r \approx 0.33$) than for $LaSrCuO_4$ ($r \approx 0.17$).[78] For this reason it is possible that t_{pa} increases with increasing r, i.e., that the correlation reported in Ref. 78 is consistent with what one would expect on the basis of the extended ILT theory. Obviously, a careful analysis involving the details of the Cu $4s$–apical-oxygen $2p_z$ bonding is required.

Note added in proof. The TPE has been recently observed also in $SmLa_{0.8}Sr_{0.2}CuO_{4-\delta}$.[79] In Ref. 80, the issue of a possible kinetic energy change at T_c is discussed in connection with the ARPES data. Some of the anomalies we predict to occur in Tl-2201 (a charge redistribution and a change of the distance between the apical oxygens and the

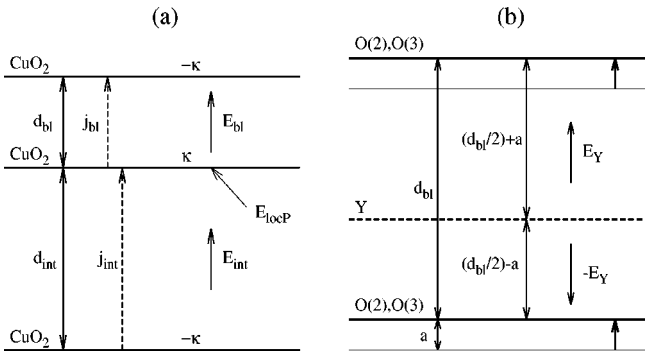

FIG. 7. (a) Schematic representation of the model. (b) The average electric field E_{bl} between the charged planes corresponding to the planar oxygens (thick horizontal lines) displaced from their equilibrium positions (thin horizontal lines) possesses a contribution ΔE_{bl} due to the charged Y plane (dashed line), $\Delta E_{bl}=[\{(d_{bl}/2)+a\}E_Y+\{(d_{bl}/2)-a\}(-E_Y)]/d_{bl}$. Here E_Y is the field due to the Y plane in the upper region of the figure. A slightly modified version of Fig. 2 from Ref. 30.

copper-oxygen planes around T_c) have been observed in x-ray diffraction studies of Tl-2212 single crystals.[81]

ACKNOWLEDGMENTS

We gratefully acknowledge discussions with D. Basov, P. Cásek, O. Dolgov, A. Dubroka, B. Farid, M. Grüninger, J. Halbritter, O. Jepsen, B. Keimer, D. van der Marel, S. Tajima, B. Velický, R. Zeyher, V. Železný, and M. L. Munzarová. We thank V. Železný for allowing us to present here the values of the intrabilayer plasma frequency of underdoped Bi-2212 prior to publication of Ref. 21. We thank O. K. Andersen for drawing our attention to Ref. 78. D.M. thanks B. Keimer for support during a stay at MPI Stuttgart, where a considerable part of the paper has been written. T.H. thanks the Alexander von Humboldt Foundation for support.

APPENDIX A: THE MAIN IDEAS OF THE MODEL OF REF. 18

Figure 7(a) shows a schematic representation of the electronic part of the model of Ref. 18. The effects related to the ionic degrees of freedom will be discussed subsequently. Thick horizontal lines correspond to the two-dimensional copper-oxygen planes. The distance between the closely spaced copper-oxygen planes forming a bilayer is denoted by d_{bl}, the distance between the bilayers is denoted by d_{int}. If an electric field E' is applied, the currents j_{bl} (intrabilayer current) and j_{int} (interbilayer current) flow between the planes. Since they are not equal, the planes become charged. The resulting surface charge density that alternates from one plane to the other is denoted by κ. It modifies the average electric field in the intrabilayer region, $E_{bl}=E'+(\kappa/\varepsilon_0\varepsilon_\infty)$, whereas it does not change the average electric field in the interbilayer region, $E_{int}=E'$. The currents j_{bl} and j_{int} are determined by the fields E_{bl} and E_{int}, respectively, $j_{bl}=\sigma_{bl}E_{bl}$ and $j_{int}=\sigma_{int}E_{int}$, so that a self-consistent set of equations is obtained. Here σ_{bl} and σ_{int} are the intrabilayer and the interbilayer conductivities, respectively. The equations can be readily solved yielding the following formula for the macroscopic dielectric function:

$$\varepsilon(\omega)=(d_{bl}+d_{int})\Big/\left[\frac{d_{bl}}{\varepsilon_{bl}(\omega)}+\frac{d_{int}}{\varepsilon_{int}(\omega)}\right]. \tag{A1}$$

Here $\varepsilon_{bl}(\omega)=(i/\varepsilon_0\omega)\sigma_{bl}(\omega)$ and $\varepsilon_{int}(\omega)=(i/\varepsilon_0\omega)\sigma_{int}(\omega)$. For a superlattice of intrabilayer and interbilayer Josephson junctions we have $\varepsilon_{bl}(\omega)=\varepsilon_\infty-(\omega_{bl}^2/\omega^2)$ and $\varepsilon_{int}(\omega)=\varepsilon_\infty-(\omega_{int}^2/\omega^2)$. The dielectric function of Eq. (A1) then exhibits two conventional plasma resonances at $\omega=\omega_{bl}/\sqrt{\varepsilon_\infty}$ and at $\omega=\omega_{int}/\sqrt{\varepsilon_\infty}$. In addition, it exhibits a pole at

$$\omega=\omega_p=\sqrt{\frac{d_{bl}\omega_{int}^2+d_{int}\omega_{bl}^2}{(d_{bl}+d_{int})\varepsilon_\infty}}, \tag{A2}$$

corresponding to a resonant oscillation of the condensate density between the two closely spaced copper-oxygen planes (transverse plasma excitation). The spectral weight of the δ peak at $\omega=0$ is

$$S_\delta=(\pi/2)\varepsilon_0\frac{(d_{bl}+d_{int})\omega_{bl}^2\omega_{int}^2}{d_{bl}\omega_{int}^2+d_{int}\omega_{bl}^2}, \tag{A3}$$

and the spectral weight of the resonance at ω_p is

$$S_{pl}=(\pi/2)\varepsilon_0\frac{d_{bl}d_{int}(\omega_{bl}^2-\omega_{int}^2)^2}{(d_{bl}+d_{int})(d_{bl}\omega_{int}^2+d_{int}\omega_{bl}^2)}. \tag{A4}$$

Equations (A1) and (A2) have been previously derived in another way by Van der Marel and Tsvetkov[12] (see also Ref. 19). As far as only the electronic degrees of freedom are concerned, the two approaches yield completely equivalent results. However, the present approach can be more easily extended to incorporate the phonons.

Assume for a moment that the displacements of the ions do not modify the electric fields E_{bl} and E_{int}. The ions located in the intrabilayer and in the interbilayer regions experience then the electric fields E_{bl} and E_{int}, respectively. The ions located in the copper-oxygen planes experience a field E_{locP} that is equal to the average of the two fields, $E_{locP}=(E_{bl}+E_{int})/2$. This can be easily explained using Fig. 7(a). Let us consider, e.g., the ions in the middle copper-oxygen plane. They experience the applied field E' and the electric field generated by the charge density $-\kappa$ of the upper copper-oxygen plane (the contributions of the other planes cancel each other). The total electric field acting on these ions is then $E_{locP}=E'+(\kappa/2\varepsilon_0\varepsilon_\infty)=(E_{bl}+E_{int})/2$. Even this simplified picture of the electric fields acting on the ions allows us to explain the spectral weight anomalies. The spectacular reduction of the spectral weight of the 320 cm^{-1} phonon mode in underdoped Y123 shown in Fig. 1, e.g., is due to the fact that in the frequency region around the phonon the two fields E_{bl} and E_{int} have opposite signs (see Ref. 18 for a discussion).

In reality, the displacements of the ions modify the electric fields E_{bl} and E_{int}, so that the model equations become slightly more complicated. As an example, we show in Fig. 7(b), how the displacement of the planar oxygens of Y123 [O(2) and O(3)] from their equilibrium position influences the electric field E_{bl}. We refer the reader to Refs. 18 and 30 for further details of the model.

APPENDIX B: APPROXIMATE ''TIGHT-BINDING'' SUM RULE FOR BILAYER COMPOUNDS

In this appendix we put the conclusions of Sec. IV B on a more rigorous basis and we present a way of estimating the contribution of the countereffects.[55] We shall discuss a microscopic counterpart of the model outlined in Appendix A. For this reason, it may be helpful for the reader to follow Fig. 7. Let us consider a model defined by the following Hamiltonian

$$H=H_{in\text{-}plane}+H_{bl}+H_{int}, \tag{B1}$$

where $H_{in\text{-}plane}$ contains the intraplanar single-particle terms and interaction terms, H_{bl} and H_{int} contain the hopping terms between the closely-spaced copper-oxygen planes and between the widely spaced ones, respectively,

$$H_{bl}=-t_{\perp\, bl}\sum_{l=1,3,5,\ldots;i;s} c^{+}_{i,l+1,s}c_{i,l,s}+\text{H.c.}, \tag{B2}$$

$$H_{int}=-t_{\perp\, int}\sum_{l=2,4,6,\ldots;i;s} c^{+}_{i,l+1,s}c_{i,l,s}+\text{H.c.} \tag{B3}$$

In the presence of an electric field along the c axis, the Hamiltonian reads

$$H_A=H-Na^2\sum_{l=1,3,5,\ldots,}\left(d_{bl}j^p(l)A_{bl}+\frac{e^2d_{bl}^2}{2a^2\hbar^2}k(l)A_{bl}^2\right)$$
$$-Na^2\sum_{l=2,4,6,\ldots}\left(d_{int}j^p(l)A_{int}+\frac{e^2d_{int}^2}{2a^2\hbar^2}k(l)A_{int}^2\right). \tag{B4}$$

Here

$$j^p(l)=\frac{iet_{\perp\alpha}}{Na^2\hbar}\sum_{i,s}(c^{+}_{i,l+1,s}c_{i,l,s}-c^{+}_{i,l,s}c_{i,l+1,s}), \tag{B5}$$

where $\alpha=bl$ for $l\in\{1,3,5,\ldots\}$ and $\alpha=int$ for $l\in\{2,4,6,\ldots\}$, are the c-axis paramagnetic current densities. Further,

$$k(l)=-\frac{t_{\perp\alpha}}{N}\sum_{i,s}(c^{+}_{i,l+1,s}c_{i,l,s}+c^{+}_{i,l,s}c_{i,l+1,s}) \tag{B6}$$

are the c-axis kinetic energies (per unit cell), N is the number of lattice sites in one copper-oxygen plane, A_{bl} is the vector potential in the intrabilayer region ($A_{bl}=E_{bl}/i\omega$), A_{int} is the vector potential in the interbilayer region ($A_{int}=E_{int}/i\omega$). When studying the optical response of the system, self-consistent values of these two vector potentials have to be used (random-phase approximation). Using similar manipulations as in Ref. 50, we obtain the following relation between the averaged total current densities j_α and the two electric fields E_α,

$$j_\alpha=\sigma_{\alpha,\beta}E_\beta. \tag{B7}$$

Here

$$j_\alpha=\left\langle j^p(l)+\frac{e^2d_\alpha^2A_\alpha}{\hbar^2a^2d_\alpha}k(l)\right\rangle, \tag{B8}$$

where $l=1$ for $\alpha=bl$ and $l=2$ for $\alpha=int$. Note that all intrabilayer regions are identical and all interbilayer regions are identical, the long-wavelength limit is assumed. Finally the four conductivities $\sigma_{\alpha,\beta}$ ($\alpha,\beta\in\{bl,int\}$) are given as follows:

$$\sigma_{\alpha,\beta}(\omega)=\frac{\langle k(l)\rangle e^2d_\alpha\delta_{\alpha,\beta}/(\hbar^2a^2)+Na^2d_\alpha\Lambda_{\alpha,\beta}(\omega)}{i(\omega+i\delta)}. \tag{B9}$$

Here

$$\Lambda_{\alpha,\beta}(\omega)=\frac{i}{\hbar}\sum_{l'}\int_{-\infty}^{\infty}d(t-t')\langle[j^p(l,t),j^p(l',t')]\rangle$$
$$\times\Theta(t-t')e^{i\omega(t-t')}, \tag{B10}$$

where $l=1$ for $\alpha=bl$ and $l=2$ for $\alpha=int$; the sum runs over the odd values of l' for $\beta=bl$ and over the even values of l' for $\beta=int$. We are not going to discuss the general case here. Instead we concentrate on the case where $t_{\perp int}\ll t_{\perp bl}$, i.e., the case of negligible interbilayer kinetic energy $\langle k(2)\rangle$. In this case we can neglect $\sigma_{bl,int}$, $\sigma_{int,bl}$, and $\sigma_{int,int}$ and we have $j_{bl}\approx\sigma_{bl,bl}E_{bl}$, $j_{int}\approx 0$. The current-current correlation functions of Eq. (B10) have the analytic properties required for the validity of the sum rules and we obtain

$$\int_0^\infty\sigma_{bl}(\omega)\,d\omega=-\frac{\pi e^2d_{bl}}{2\hbar^2a^2}\langle k(1)\rangle, \tag{B11}$$

where $\sigma_{bl}(\omega)\equiv\sigma_{bl,bl}(\omega)$. The sum rule (B11) yields a formula for the change of the kinetic energy upon entering the superconducting state analogous to Eq. (8) or Eq. (10) [$\sigma(\omega)$ is substituted by $\sigma_{bl}(\omega)$ and d is substituted by d_{bl}]. For vanishingly small values of the regular part of σ_{bl}, we obtain $\Delta\langle k(1)\rangle\ [\text{meV}]=-4C(\omega_{bl}\ [\text{cm}^{-1}])^2/d_{bl}\ [\text{Å}]$. This is nothing else than Eq. (3) except for the factor of 4.[56] In a general case, Eq. (11) yields a recipe for how to treat the countereffects.

*Permanent address: IFD, Warsaw University, Hoza, 69, PL-00-681 Warsaw, Poland.

[1] S. Chakravarty, A. Sudbo, P. W. Anderson, and S. Strong, Science **261**, 337 (1993).

[2] P. W. Anderson, *The Theory of Superconductivity in the High-T_c Cuprates* (Princeton University Press, Princeton, NJ, 1997).

[3] N. Kumar, T. P. Pareek, and A. M. Jayannavar, Phys. Rev. B **57**, 13 399 (1998), and references therein.

[4] S. Chakravarty, Eur. Phys. J. B **5**, 337 (1998).

[5] P. W. Anderson, Science **279**, 1196 (1998).

[6] J. Schützmann, H. S. Somal, A. A. Tsvetkov, D. van der Marel, G. E. J. Koops, N. Koleshnikov, Z. F. Ren, J. H. Wang, E. Brück, and A. A. Menovsky, Phys. Rev. B **55**, 11 118 (1997). The value of E_J of slightly underdoped $La_{2-x}Sr_xCuO_4$ reported in this work is by a factor of ~ 5 lower than an estimate of U_0. For $Tl_2Ba_2CuO_6$, $E_J < 0.005U_0$.

[7] K. A. Moler, J. R. Kirtley, D. G. Hinks, T. W. Li, and M. Xu, Science **279**, 1193 (1998).

[8] A. A. Tsvetkov, D. van der Marel, K. A. Moler, J. R. Kirtley, D. Dulic, A. Damascelli, M. Grüninger, J. Schützmann, J. W. van der Eb, H. S. Somal, J. L. de Boer, A. Meetsma, N. Koleshnikov, Z. F. Ren, and J. H. Wang, Nature (London) **395**, 360 (1998).

[9] D. Dulic, D. van der Marel, A. A. Tsvetkov, W. N. Hardy, Z. F. Ren, J. H. Wang, and B. A. Willemsen, Phys. Rev. B **60**, R15 051 (1999).

[10] J. R. Kirtley, K. A. Moller, G. Villard, and A. Maignan, Phys. Rev. Lett. **81**, 2140 (1998).

[11] P. W. Anderson, Science **268**, 1154 (1995).

[12] D. van der Marel and A. Tsvetkov, Czech. J. Phys. **46**, 3165 (1996). A detailed calculation of the dielectric function in superconductors consisting of two Josephson coupled superconducting layers per unit cell, taking into account the effect of finite compressibility of the electron fluid, is presented in the following preprint: D. van der Marel and A. A. Tsvetkov, cond-mat/0102411 (unpublished).

[13] D. van der Marel *et al.* (private communication).

[14] C. C. Homes, T. Timusk, D. A. Bonn, R. Liang, and W. N. Hardy, Phys. Rev. Lett. **71**, 1645 (1993).

[15] C. C. Homes, T. Timusk, D. A. Bonn, R. Liang, and W. Hardy, Physica C **254**, 265 (1995), and references therein.

[16] J. Schützman, S. Tajima, S. Miyamoto, Y. Sato, and R. Hauff, Phys. Rev. B **52**, 13 665 (1995).

[17] C. Bernhard, D. Munzar, A. Golnik, C. T. Lin, A. Wittlin, J. Humlíček, and M. Cardona, Phys. Rev. B **61**, 618 (2000), and references therein.

[18] D. Munzar, C. Bernhard, A. Golnik, J. Humlíček, and M. Cardona, Solid State Commun. **112**, 365 (1999).

[19] M. Grüninger, D. Van der Marel, A. A. Tsvetkov, and A. Erb, Phys. Rev. Lett. **84**, 1575 (2000); M. Grüninger, Ph.D. thesis, University of Groningen, Netherlands, 1999.

[20] V. Železný, S. Tajima, T. Motohashi, J. Shimoyama, K. Kishio, and D. van der Marel, J. Low Temp. Phys. **117**, 1019 (1999).

[21] V. Železný, S. Tajima, D. Munzar, T. Motohashi, J. Shimoyama, and K. Kishio, Phys. Rev. B **63**, 060502 (2001).

[22] J. W. Loram, K. A. Mirza, and J. R. Cooper (unpublished).

[23] J. W. Loram, J. Luo, J. R. Cooper, W. Y. Liang, and J. L. Tallon, J. Phys. Chem. Solids **62**, 59 (2001).

[24] S. Chakravarty, H. Kee, and E. Abrahams, Phys. Rev. Lett. **82**, 2366 (1999).

[25] D. N. Basov, S. I. Woods, A. S. Katz, E. J. Singley, R. C. Dynes, M. Xu, D. G. Hinks, C. C. Homes, and M. Strongin, Science **283**, 49 (1999).

[26] D. van der Marel, A. Tsvetkov, M. Grüninger, D. Dulic, and H. J. A. Molegraaf, Physica C **341**, 1531 (2000).

[27] A. Wittlin, R. Liu, M. Cardona, L. Genzel, W. König, and F. Garcia-Alvarado, Solid State Commun. **64**, 477 (1987).

[28] A. P. Litvinchuk, C. Thomsen, and M. Cardona, in *Physical Properties of High Temperature Superconductors IV*, edited by D. M. Ginsberg (World Scientific, Singapore, 1994), p. 375 and references therein.

[29] S. Kamba, J. Petzelt, V. Železný, E. V. Pechen, S. I. Krasnosvobodtsev, and B. P. Gorschunov, Solid State Commun. **70**, 547 (1989).

[30] D. Munzar, C. Bernhard, A. Golnik, J. Humlíček, and M. Cardona, J. Low Temp. Phys. **117**, 1049 (1999).

[31] J. Humlíček, A. P. Litvinchuk, W. Kress, B. Lederle, C. Thomsen, M. Cardona, H. U. Habermeier, I. E. Trofimov, and W. König, Physica C **206**, 345 (1993).

[32] W. Kress (private communication).

[33] R. Henn, T. Strach, E. Schönherr, and M. Cardona, Phys. Rev. B **55**, 3285 (1997).

[34] C. Bernhard, R. Henn, A. Wittlin, M. Kläser, Th. Wolf, G. Müller Vogt, C. T. Lin, and M. Cardona, Phys. Rev. Lett. **80**, 1762 (1998).

[35] A. P. Litvinchuk, C. Thomsen, M. Cardona, J. Karpinski, E. Kaldis, and S. Rusiecki, Z. Phys. B: Condens. Matter **92**, 9 (1993).

[36] D. N. Basov, T. Timusk, B. Dabrowski, and J. D. Jorgensen, Phys. Rev. B **50**, 3511 (1994).

[37] M. Reedyk, T. Timusk, Y. W. Hsueh, B. W. Statt, J. S. Xue, and J. E. Greedan, Phys. Rev. B **56**, 9129 (1997).

[38] C. Bernhard, T. Holden, A. Golnik, C. T. Lin, and M. Cardona, Phys. Rev. B **62**, 9138 (2000).

[39] A. V. Boris, P. Mandal, C. Bernhard, N. N. Kovaleva, K. Pucher, J. Hemberger, A. Loidl, cond-mat/0012510 (unpublished).

[40] T. Zetterer, M. Franz, J. Schützmann, W. Ose, H. H. Otto, and K. F. Renk, Phys. Rev. B **41**, 9499 (1990).

[41] J. Prade, A. D. Kulkarni, F. W. de Wette, U. Schröder, and W. Kress, Phys. Rev. B **39**, 2771 (1989).

[42] S. Tajima, G. D. Gu, S. Miyamoto, A. Odagawa, and N. Koshizuka, Phys. Rev. B **48**, 16 164 (1993). The broadening of the 600 cm^{-1} phonon mode apparent in Fig. 3 of this paper may correspond to the additional spectral weight identified in our investigations.

[43] H. Shibata and A. Matsuda, Phys. Rev. B **59**, 11 672 (1999), and references therein.

[44] For Bi-2212, $\alpha = -[n_{Ca}e^*_{Ca} + (n_{Cu}e^*_{Cu}/2)](d_{bl}+d_{int})/(n_{O(1)}e^*_O\, d_{bl})$, $\beta = -[n_{Bi}e^*_{Bi} + n_{O(3)}e^*_O + n_{Ba}e^*_{Ba} + n_{O(2)}e^*_O + (n_{Cu}e^*_{Cu}/2)](d_{bl}+d_{int})/(n_{O(1)}e^*_O\, d_{int})$, and $\gamma = (d_{bl}+d_{int})/d_{int}$, where, e.g., n_{Ca} is the number of Ca ions per unit cell, O(1) denotes the planar oxygen, O(3) the BiO-layer oxygen, and O(2) the apical oxygen. For Tl-2201, $\alpha = -[n_{Ba}e^*_{Ba} + n_{O(3)}e^*_O + n_{Cu}e^*_{Cu}](d_A+d_B)/(n_{O(2)}e^*_O\, d_A) = 1.1$, $\beta = -[n_{Tl}e^*_{Tl} + n_{O(1)}e^*_O](d_A+d_B)/(n_{O(2)}e^*_O\, d_B) = 0.9$, and $\gamma = (d_A+d_B)/d_B = 1.8$, where O(1) denotes the TlO-layer oxygen, O(2) the apical oxygen, and O(3) the planar oxygen. These values correspond to the case where the region A is considered as ''intrabilayer.'' In the other case (A is considered as ''interbilayer'') the value of α (β) corresponds to the above value of β (α) and $\gamma = (d_A+d_B)/d_A = 2.2$.

[45] M. Tinkham and R. A. Ferrel, Phys. Rev. Lett. **2**, 331 (1959); M. Tinkham, *Introduction to Superconductivity* (McGraw-Hill, New York, 1996), Chap. 3.9.3.

[46] The formula is equivalent to formula (5) of Ref. 5 or formula (1) of Ref. 6. It differs by a factor of 4 from formula (4) of Ref. 4.

[47] The values of ω_{bl} can be simply guessed from the data by inserting the frequency of the transverse plasma excitation into Eq. (A2) and using an estimate of ε_∞. However, the plasma fre-

quency is screened not only by the interband processes contributing to ε_∞ but also by mid-infrared processes. The description of the contribution of these processes contains a certain degree of arbitrarness. In particular, when fitting the infrared data, one has to make some assumptions concerning the frequency dependence of this contribution and concerning its distribution between the intrabilayer and interbilayer regions. Note that the assumptions made in Ref. 18 are different from those made in Ref. 19.

[48] In Ref. 18 we have suggested that the onset of the anomalies above T_c can be explained by assuming that the intrabilayer plasmon starts to develop already below $T^* > T_c$. There is no global phase coherence above T_c and consequently, strictly speaking, no Josephson effects. It can be speculated, however, that above T_c there is either a certain degree of phase coherence between the closely spaced copper-oxygen planes or at least some kind of pairing developed making a (semi)coherent intrabilayer hopping possible.

[49] H. Ehrenreich, in *The Optical Properties of Solids*, Proceedings of the International School of Physics ''Enrico Fermi,'' Course XXXIV, Varenna, 1965, edited by J. Tauc (Academic Press, New York, 1966).

[50] D. J. Scalapino, S. R. White, and S. C. Zhang, Phys. Rev. Lett. **68**, 2830 (1992).

[51] F. L. Pilar, *Elementary Quantum Chemistry* (McGraw-Hill, New York, 1968).

[52] O. K. Andersen, A. Lichtenstein, O. Jepsen, and F. Paulsen, J. Phys. Chem. Solids **56**, 1573 (1995).

[53] This scale corresponds to the frequency range where the single-particle tunneling is completely blocked.

[54] In reality, the regions of intraband and interband absorption overlap. Considering this would make the discussion more complicated, while it would not change our main conclusions.

[55] The contribution to the *c*-axis kinetic energy due to the single-particle tunneling may increase below T_c; that is what we mean by ''countereffects.''

[56] For a given plasma frequency of the condensate (or, alternatively, for a given penetration depth) the sum-rule-based approach of Refs. 4 and 24 [Eq. (8)] yields a change of the *c*-axis kinetic energy by a factor of 4 larger than Eq. (3) if the changes of the regular part of $\sigma_1(\omega)$ between the normal and the superconducting state are negligible. For underdoped $La_{2-x}Sr_xCuO_4$ this discrepancy is partially reduced because of the changes in the background.

[57] G. Hastreiter, U. Hofmann, J. Keller, and K. F. Renk, Solid State Commun. **76**, 1015 (1990); G. Hastreiter and J. Keller, *ibid.* **85**, 967 (1993).

[58] L. B. Ioffe and A. J. Millis, Phys. Rev. B **61**, 9077 (2000), and references therein. The authors suggest that the additional peak corresponds to a pair-breaking excitation in the absence of complete phase coherence.

[59] R. Zeyher (private communication).

[60] This is particularly clear in the case of underdoped Y123 with $T_c = 53$ K [see Fig. 1(a)]. Both the additional peak and the anomaly of the 320 cm^{-1} phonon mode can be fitted using only three essential parameters: ω_{bl}, S_P (oscillator strength of the phonon) and ω_P (frequency of the phonon).

[61] A. A. Tsvetkov, D. Dulic, D. van der Marel, A. Damascelli, G. A. Kaljushnaia, J. I. Gorina, N. N. Senturina, N. N. Kolesnikov, Z. F. Ren, J. H. Wang, A. A. Menovsky, and T. T. M. Palstra, Phys. Rev. B **60**, 13 196 (1999).

[62] A. S. Katz, S. I. Woods, E. J. Singley, T. W. Li, M. Xu, D. G. Hinks, R. C. Dynes, and D. N. Basov, Phys. Rev. B **61**, 5930 (2000).

[63] Y. Shimakawa, Y. Kubo, T. Manako, Y. Nakabayashi, and H. Igarashi, Physica C **156**, 97 (1988).

[64] A. D. Kulkarni, F. W. de Wette, J. Prade, U. Schröder, and W. Kress, Phys. Rev. B **41**, 6409 (1990).

[65] It is surprising that the Tl-layer-oxygen mode exhibits the anomalies rather than the apical-oxygen mode (the apical-oxygen plane forms a boundary between the regions A and B in the same way as the plane of the planar oxygens in Y123 forms a boundary between the intrabilayer and the interbilayer regions). The reason is that the geometry is different. In Y123, $d_{int} \gg d_{bl}$, here $d_A \approx d_B$.

[66] The values of the model conductivity in the frequency region around 800 cm^{-1} are by a factor of ~ 2 higher than the value of $\sim 10\ \Omega^{-1}\ cm^{-1}$ reported in Ref. 25. This is not a serious discrepancy considering the oversimplified ansatz for σ_A and σ_B.

[67] The value of the condensation energy of Tl-2201 can be estimated using the specific-heat data presented in J. M. Wade, J. W. Loram, K. A. Mirza, J. R. Cooper, and J. L. Tallon, J. Supercond. **7**, 261 (1994). The value of $\delta\gamma(T_c)$ is by a factor of ~ 3 smaller than that for optimally doped Y123 suggesting $U_0 \approx 0.1$ meV.

[68] C. Bernhard *et al.* (unpublished).

[69] E. Janod, R. Calemczuk, J.-Y. Henry, and C. Marcenat, Phys. Lett. A **205**, 105 (1995).

[70] E. Nyeanchi, D. F. Brewer, T. E. Hargreaves, A. L. Thompson, C. Liezhao, and C. Zhao-Jia, Physica C **235**, 1755 (1994).

[71] M. Merz, N. Nücker, P. Schweiss, S. Schuppler, C. T. Chen, V. Chakarian, J. Freeland, Y. U. Idzerda, M. Kläser, G. Müller-Vogt, and Th. Wolf, Phys. Rev. Lett. **80**, 5192 (1998).

[72] O. V. Misochko, E. Ya. Sherman, N. Umesaki, K. Sakai, and S. Nakashima, Phys. Rev. B **59**, 11 495 (1999).

[73] M. Sardar, Physica C **298**, 254 (1998).

[74] J. Halbritter, J. Supercond. **11**, 231 (1998).

[75] P. Penzi, D. Schild, and J. Halbritter (unpublished).

[76] Ch. Chelm, Ch. Preis, F. Forsthofer, J. Keller, K. Schlenga, R. Kleiner, and P. Müller, Phys. Rev. Lett. **79**, 737 (1997); Ch. Chelm, Ch. Preis, Ch. Walter, and J. Keller, Phys. Rev. B **62**, 6002 (2000).

[77] T. Koyama, Physica C **341**, 1381 (2000); T. Koyama (unpublished).

[78] E. Pavarini, I. Dasgupta, T. Saha-Dasgupta, O. Jepsen, and O. K. Andersen, cond-mat/0012051 (unpublished).

[79] H. Shibata, Phys. Rev. Lett., **86**, 2122 (2001); T. Kakeshita, S. Uchida, K. M. Kojima, S. Adachi, B. Gorshunov, and M. Dressel, *ibid.* **86**, 4140 (2001); D. Dulic, A. Pimenov, D. van der Marel, D. M. Broun, S. Kamal, W. N. Hardy, A. A. Tsvetkov, I. M. Sutjaha, R. Liang, A. A. Menovsky, A. Loidl, and S. S. Saxena, *ibid.* **86**, 4144 (2001).

[80] M. R. Norman, M. Randeira, B. Jankó, and J. C. Campuzano, Phys. Rev. B, **61**, 14 742 (2000).

[81] S. Sasaki, T. Mori, K. Kawaguchi, and M. Nakao, Physica C **247**, 289 (1995); V. N. Molchanov and V. I. Simonov, Acta Crystallogr., Sect. A: Found. Crystallogr. **A54**, 905 (1998)